EPJ E
Soft Matter and Biological Physics
EPJ.org
your physics journal

Eur. Phys. J. E **29**, 305–310 (2009) DOI: 10.1140/epje/i2009-10478-6

Evidence of a two-state picture for supercooled water and its connections with glassy dynamics

G.A. Appignanesi, J.A. Rodriguez Fris and F. Sciortino

EDP SCIENCES
Società Italiana di Fisica
Springer

Eur. Phys. J. E **29**, 305–310 (2009)
DOI 10.1140/epje/i2009-10478-6

THE EUROPEAN PHYSICAL JOURNAL E

Regular Article

Evidence of a two-state picture for supercooled water and its connections with glassy dynamics

G.A. Appignanesi[1], J.A. Rodriguez Fris[1,a], and F. Sciortino[2]

[1] Área de Fisicoquímica, Departamento de Química and INQUISUR, Universidad Nacional del Sur, Avenida Alem 1253, 8000 Bahía Blanca, Argentina
[2] Dipartimento di Fisica and INFM-CNR-SOFT, Università di Roma "La Sapienza", Piazzale A. Moro 2, 00185 Roma, Italy

Received 4 March 2009
Published online: 16 July 2009 –

Abstract. The picture of liquid water as consisting of a mixture of molecules of two different structural states (structured, low-density molecules and unstructured, high-density ones) represents a belief that has been around for long time awaiting for a conclusive validation. While in the last years some indicators have indeed provided certain evidence for the existence of structurally different "species", a more definite bimodality in the distribution function of a sound structural quantity would be desired. In this context, our present work combines the use of a structural parameter with a minimization technique to yield neat bimodal distributions in a temperature range within the supercooled liquid regime, thus clearly revealing the presence of two populations of differently structured water molecules. Furthermore, we elucidate the role of the inter-conversion between the identified two kinds of states for the dynamics of structural relaxation, thus linking structural information to dynamics, a long-standing issue in glassy physics.

PACS. 61.20.Ja Computer simulation of liquid structure – 61.20.Lc Time-dependent properties; relaxation – 61.25.Em Molecular liquids

1 Introduction

The study of structural and dynamical properties of water is essential for several research areas, encompassing solvation, reaction dynamics and biology and for understanding the several anomalies which characterize this liquid and which become more conspicuous as it is supercooled below its melting temperature [1–4]. Such anomalies have been tentatively associated to the presence of two competing preferential local structures, identified with molecules characterized by high or low local density [2, 5, 6]. Support for this idea comes from the existence of at least two different forms of amorphous glass states, namely low-density amorphous ice LDA and (very) high-density amorphous ice (V)HDA [7–10]. Here we show that a sophisticated analysis of simulation data provides a clear evidence that supercooled water is indeed a mixture of domains of two kinds of molecules and that the interconversion between these two "species" is at the heart of the dynamical events responsible for the structural (or α) relaxation. In turn, analysis of experiments and simulation data of glass-forming liquids has shown that dynamics close to the glass transition is characterized by the presence of dynamical heterogeneities [11–13], *i.e.* by significant differences in the mobility of different spatial regions of the system. The memory of the initial structure is lost in a time, named structural (or α) relaxation time τ_α, which increases significantly upon supercooling. Simulation studies have shown that such relaxation is performed by means of rapid cooperatively relaxing events which drive the system from one metabasin (group of similar structures) to another [14,15]. However, connections between static and dynamic properties in glass-forming liquids have been elusive, despite the significant amount of work devoted to this topic [16–18], probably due to the similarities in the local arrangements of the different particles composing the liquid. In the case of supercooled water, dynamical studies [19] have shown that the slowing down of the dynamics is consistent with the general heterogeneous scenario of glassy relaxation alluded before by presenting spatial regions with dynamics that vary drastically from one to another. The size of such regions of cooperatively moving particles, consisting of compact clusters of mobile molecules [19], is expected to grow significantly upon cooling. Again little information is presently available on the connections between dynamic properties of these clusters and changes in the local structural properties.

It is thus important i) to properly identify an efficient indicator which enables the classification of molecules according to their local structural properties and ii) to

[a] e-mail: rodriguezfris@plapiqui.edu.ar

establish a link between structure and dynamics by connecting the loss of memory which takes place during the α relaxation to the presence and to the dynamics of domains of differently structured molecules.

2 Detecting molecules with different local structures

In order to find molecules participating in the dynamical events responsible for the α relaxation, we must study a small system, *i.e.* of $N = 216$ water molecules so that independent events can be properly identified. These molecules interact via the Simple Point Charge (Extended) potential (SPC/E) [20] in a cubic box at density $1.0\,\mathrm{g/cm^3}$, using periodic boundary conditions, in the T range from 260 K to 200 K. Long-range interactions have been modeled via reaction field. At the lowest T we simulate a trajectory of 400 ns. At this T the α-relaxation time, defined as the time at which the self-intermediate scattering function at wave number $18\,\mathrm{nm^{-1}}$ reaches the value $1/e$, is 8.5 ns. Even when most of the results we shall show are for $T = 210\,\mathrm{K}$ and density $1.0\,\mathrm{g/cm^3}$, we have found qualitatively the same behavior within the temperature range (in the supercooled regime) above indicated. Additionally, similar results are produced when the density is decreased to $0.9\,\mathrm{g/cm^3}$.

To study the local structure of water molecules on a quantitative basis, we use the indicator, proposed by Shiratani and Sasai [5,6], which associates a local structure index (LSI) to each molecule to quantify the degree of local order. The key observation is the existence of certain molecules which show an unoccupied gap between 3.2 Å and 3.8 Å in their radial neighbor distribution for certain periods of time. Such low-density molecules are well structured and coordinated in a highly tetrahedral manner with other four water molecules. Occupancy of such gap increases the local density and distorts the tetrahedral order of the central molecule. Shiratani and Sasai [5,6] defined LSI $= I(i,t)$ for molecule i at time t. For each molecule i, one orders the rest of the molecules depending on the radial distance r_j between the oxygen of the molecule i and the oxygen of molecule j: $r_1 < r_2 < r_j < r_{j+1} < \ldots < r_{n(i,t)} < r_{n(i,t)+1}$, $n(i,t)$ is chosen so that $r_{n(i,t)} < 3.7\,\text{Å} < r_{n(i,t)+1}$. Then, $I(i,t)$ is defined as [5,6]

$$I(i,t) = \frac{1}{n(i,t)} \sum_{j=1}^{n(i,t)} \left[\Delta(j;i,t) - \overline{\Delta}(i,t)\right]^2,$$

where $\Delta(j;i,t) = r_{j+1} - r_j$ and $\overline{\Delta}(i,t)$ is the average over all molecules of $\Delta(j;i,t)$. Thus, $I(i,t)$ expresses the inhomogeneity in the radial distribution within the sphere of radius around 3.7 Å. A high value of $I(i,t)$ implies that the molecule i at time t is characterized by a tetrahedral local order and a low-local density, while on the contrary, values of $I(i,t) \approx 0$ indicate a molecule with defective tetrahedral order and high-local density. Differently from refs. [5,6], we calculate such index in the inherent structures IS (minimizing the potential energy of the corresponding instantaneous structure) to filter out the randomizing effect introduced by the thermal vibrations [21], effectively removing the fluctuations present in the real trajectory which hamper the possibility of properly identifying the local structure.

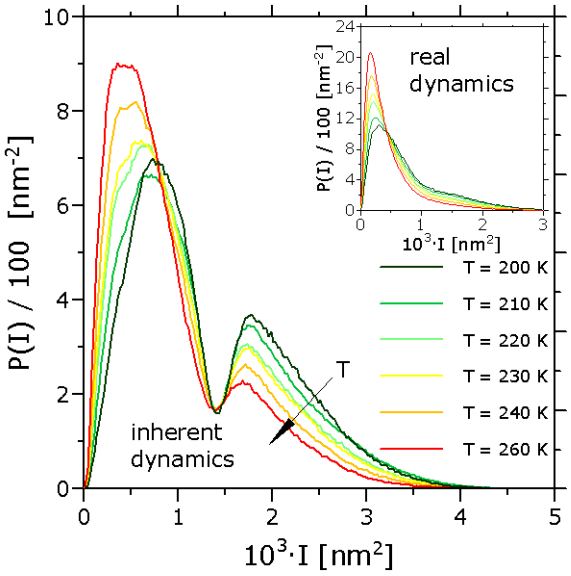

Fig. 1. Probability density $P(I)$ of finding a molecule with local structure index I for six temperatures (200 K, 210 K, 220 K, 230 K, 240 K and 260 K). All curves cross at the same $I_{\min} \approx 1.4 \cdot 10^{-3}\,\mathrm{nm^2}$. The inset shows the same curves evaluated in the real trajectory. Note that, in this last case, no clear separation in the two populations is observable.

Figure 1 shows the distribution of $I(i,t)$ in the range $200\,\mathrm{K} \le T \le 260\,\mathrm{K}$. Direct inspection of such figure shows a new relevant result: for all temperatures studied the distribution —evaluated in the IS— is clearly bimodal. The left peak (whose amplitude decreases as T decreases) is indicative of unstructured (high-density) water molecules while the right peak (whose amplitude increases as T decreases) marks the presence of highly structured (low-density) molecules. It is important to notice that the position of the minimum (abscissa: $I_{\min} \approx 1.4 \cdot 10^{-3}\,\mathrm{nm^2}$) that separates the two peaks is invariant for all studied temperatures (a kind of "isosbestic point"), a strong indication of the existence of two populations with well-characterized local structures in dynamical equilibrium and whose relative concentration changes with T. This finding clearly supports a picture of supercooled water consisting of a mixture of molecules in two structural states, the fraction of structured molecules increasing as T is lowered. We also note that other indicators of local structure (which like the LSI have indeed provided first evidence for such a description), namely, the parameters q [22,23] and θ [24,25] or the total energy of the molecule [26], do not produce such clear bimodal distributions with a deep T-invariant minimum, not even at the IS level (only q and θ exhibit for some limited cases a very slight two-peak shape [23,25]

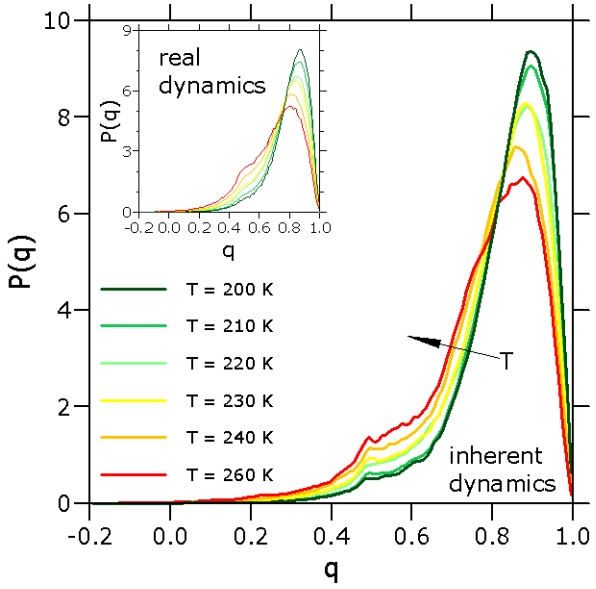

Fig. 2. Probability density $P(q)$ of finding a molecule with tetrahedral index q for six temperatures (200 K, 210 K, 220 K, 230 K, 240 K and 260 K). The inset shows the same curves evaluated in real trajectory.

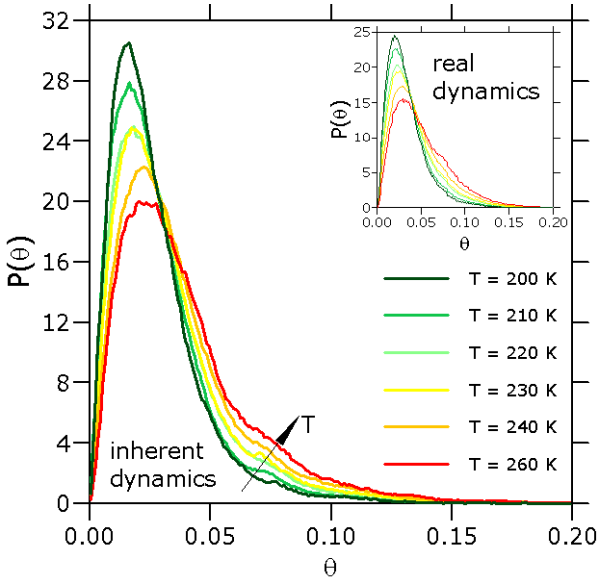

Fig. 3. Probability density $P(\theta)$ of finding a molecule with tetrahedricity index θ for six temperatures (200 K, 210 K, 220 K, 230 K, 240 K and 260 K). The inset shows the same curves evaluated in real trajectory.

but the use of the ISs does not improve the bimodality, as we show in figs. 2 and 3). The first index, the tetrahedral index q, is defined as follows:

$$q(i,t) = 1 - \frac{3}{8}\sum_{j=1}^{3}\sum_{k=j+1}^{4}\left(\frac{1}{3} + \cos\psi_{jk}(i,t)\right)^2,$$

where $\psi_{jk}(i,t)$ is the angle between the lines connecting the oxygen of molecule i with those of its nearest molecules j and k at time t. Then, $-3 \leq q(i,t) \leq 1$, and a high value indicates that molecule i has a good tetrahedral order [23]. The second index, the tetrahedricity index θ, has the following mathematical form:

$$\theta(i,t) = \frac{6\sum_{j=1}^{5}\sum_{k=j+1}^{6}[l_j(t) - l_k(t)]^2}{15\sum_{j=1}^{6} l_j^2(t)},$$

where $l_k(t)$ are the lengths of the six ($k \in \mathbb{N}$, $1 \leq k \leq 6$) edges of the tetrahedron formed by the four nearest (oxygens) neighbours from oxygen i (oxygen i is located in the center of the tetrahedron). For an ideal tetrahedron, $\theta(i,t)$ is equal to zero.

Here we show the results when the indices q and θ are applied to the same data of fig. 1. In fig. 2 we plot the q-distribution for all studied T for the inherent dynamics. The inset corresponds to the same data but evaluated in the real dynamics. Furthermore, in fig. 3 we plot the θ-distribution for the inherent dynamics, where the inset shows the same data but calculated from the real dynamics. From figs. 2 and 3, it can easily be seen that none of the curves show the neat bimodal behavior of fig. 1.

Assuming that (for any given T) the distribution of the LSI (fig. 1) is the result of the contributions of two different distributions (one for structured and the other for unstructured molecules) and given the pronounced slopes of the curve at both sides of $I_{\min} \approx 1.4 \cdot 10^{-3}\,\mathrm{nm}^2$, the overlapping between the two distributions would be quite small (at variance from the situation for the q or θ indices [23,25]). Figure 4 shows a fit providing the approximate shapes of such distributions.

3 Linking structural changes to relevant relaxation events

Having been able to clearly determine the existence of two kinds of water preferred structural states, we now attempt to connect them to dynamical heterogeneities, by studying the time evolution of the LSI. Thus we calculate the function

$$\Omega(t,\phi) = N^{-1}\sum_{i=1}^{N}|I(i,t+\phi) - I(i,t)|.$$

While the time dependence of the averaged (over all molecules) value of $I(i,t)$ does not show any significant dynamic information, the function $\Omega(t,\phi)$, by evaluating the (absolute value of the) difference of I for the same molecule i, sums the relevant changes in LSI of the single molecules in the time interval ϕ. A choice of ϕ of the order of a few percent of τ_α makes it possible to properly signal the state change. Figure 5(a) shows that the time evolution of $\Omega(t,\phi)$ (blue line) is not homogeneous in time. On the contrary, there exist certain times when the system experiences significant structural changes, as signalled by the presence of peaks.

To quantify the number of molecules showing large changes in their LSI values associated to crossing between

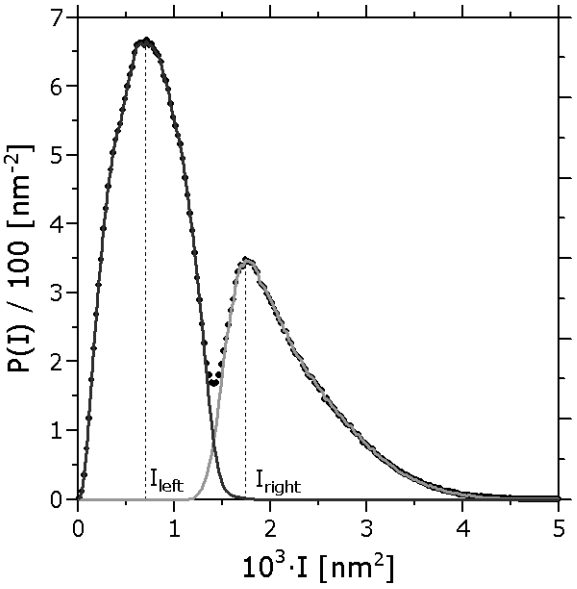

Fig. 4. An approximate decomposition of the probability density $P(I)$ of finding a molecule with local structure index I at $T = 210\,\mathrm{K}$ (dots) into two contributions: of structured (light grey line) and unstructured (dark grey line) molecules. The peak of the distribution of unstructured molecules is centered at $I_{\mathrm{left}} \approx 7 \cdot 10^{-4}\,\mathrm{nm}^2$ (where the distribution of structured molecules has already decayed), while the one for the structured molecules is centered at $I_{\mathrm{right}} \approx 18 \cdot 10^{-4}\,\mathrm{nm}^2$ (where no significant population of unstructured molecules is observed).

the two states, we count the number $N_{\mathrm{crossing}}(t,\phi)$ (red line) of molecules crossing between I_{left} and I_{right} (*i.e.* changing between the two structural states, from $I < I_{\mathrm{left}}$ to $I > I_{\mathrm{right}}$, and vice versa) in the time interval $[t, t+\phi]$ (different definitions of the crossing produce similar results). $I_{\mathrm{left}} \approx 7 \cdot 10^{-4}\,\mathrm{nm}^2$ and $I_{\mathrm{right}} \approx 18 \cdot 10^{-4}\,\mathrm{nm}^2$ correspond, respectively, to the peaks in the distribution of unstructured and structured water molecules.

We find that, on average, $\approx 5\%$ of the molecules change from a structured to a non-structured state and vice versa within the time ϕ. The time dependence of $N_{\mathrm{crossing}}(t,\phi)$, also shown in fig. 5(a), strongly correlates with the time dependence of $\Omega(t,\phi)$, supporting the view that the interconversion between the two states is the basic mechanism for structural relaxation.

Next we connect the evolution of the LSI changes with the dynamical evolution of the system to provide evidence that, in the case of water, the wide variety of local sampled structures allows for a clear detection of the existence of i) strong correlation between structural fluctuations and dynamics in the supercooled state and ii) spatial correlations in both static and dynamic quantities. Figure 5(b) shows the averaged squared displacement function [14,19]

$$\delta^2(t,\phi) = N^{-1} \sum_{i=1}^{N} \left|\mathbf{r}_i(t+\phi) - \mathbf{r}_i(t)\right|^2,$$

where $\mathbf{r}_i(t)$ is the position of the oxygen of molecule i at time t. Thus, $\delta^2(t,\phi)$ gives the system averaged squared displacement of a molecule in time interval $[t, t+\phi]$.

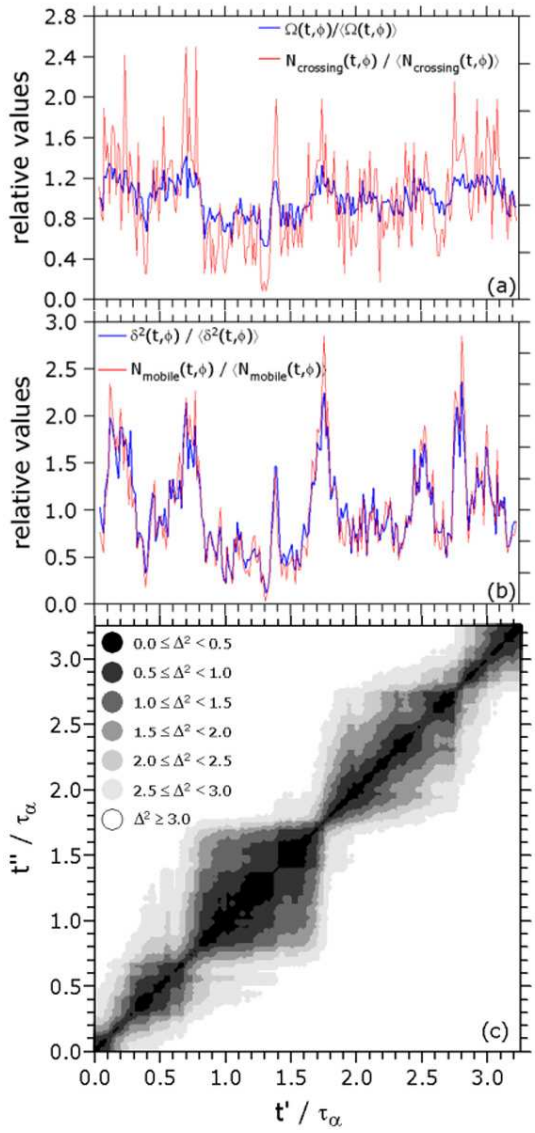

Fig. 5. (Colour on-line) Characterization of the time evolution of the water structure at $T = 210\,\mathrm{K}$: Time dependence of the functions (a) $\Omega(t,\phi)$, $N_{\mathrm{crossing}}(t,\phi)$ and (b) $\delta^2(t,\phi)$, $N_{\mathrm{mobile}}(t,\phi)$, normalized by their mean (over time) values ($\langle\ldots\rangle$ is a time average). The mean values of these functions are, respectively, 0.056 Å^2, 11.6, 0.491 Å^2 and 27.4. The value of ϕ is 40 ps. The total simulation time is 2.5 ns. $\tau_\alpha(T = 210\,\mathrm{K}) = 0.769\,\mathrm{ns}$. All data are calculated via the analysis of ISs to suppress thermal motion. An equivalent result could be obtained by performing an analysis of the real structures followed by a time average over a time comparable to the typical vibrational times. (c) Distance matrix $\Delta^2(t',t'')$ for the same trajectory. The grey level corresponds to values of $\Delta^2(t',t'')$ that are given to the left of the figure (units are Å^2). Panels (a), (b) and (c) share the same time axis.

This function (blue line) displays the typical behavior for glassy relaxation (observed also in other glassy systems like binary Lennard-Jones [14], and recently experimentally measured by means of single-molecule experiments in polymeric systems [27]). The sharp peaks indicate an enhancement in mobility which takes place in bursts, the relevant events for the structural relaxation of the sys-

tem [14,19]. This sequence of quick but sporadic motions is best grasped by the distance matrix $\Delta^2(t',t'')$ [14,28]:

$$\Delta^2(t',t'') = N^{-1}\sum_{i=1}^{N}\left|\mathbf{r}_i(t') - \mathbf{r}_i(t'')\right|^2 .$$

Therefore, $\Delta^2(t',t'')$ gives the system averaged squared displacement of a molecule in the time interval that starts at t' and ends at t''. In other words, this distance matrix contains the averaged squared distances between (the oxygens of) each recorded structure and all the other ones. Figure 5(c) shows the distance matrix, where the dark-squared islands (metabasin of the potential energy surface [14, 15, 19, 21]) indicate that the system is exploring similar structures, jumping from one metabasin to the next within a time much shorter than the time spent in each metabasin.

Figures 5(a-b) show the presence of a clear correlation between the functions $\delta^2(t,\phi)$ and $\Omega(t,\phi)$ despite the fact that $\delta^2(t,\phi)$ is based on dynamical information, that is, particle displacements, while $\Omega(t,\phi)$ relies only on local structural information. This correlation can be measured quantitatively by calculating the cross-correlation coefficient $R_{\delta^2,X} = \sum_t R(t)$ between the averaged squared displacement $\delta^2(t,\phi)$ and another observable $X(t,\phi)$:

$$R(t) = \frac{[\delta^2(t,\phi) - \langle\delta^2\rangle]}{\{\langle[\delta^2(t,\phi) - \langle\delta^2\rangle]^2\rangle\}^{1/2}} \cdot \frac{[X(t,\phi) - \langle X\rangle]}{\{\langle[X(t,\phi) - \langle X\rangle]^2\rangle\}^{1/2}} ,$$

where $\langle\ldots\rangle$ is a time average. Positive values of $R_{\delta^2,X}$ ($-1 \leq R \leq 1$) indicate that functions δ^2 and X are positively correlated while negative values indicate anti-correlation and values close to zero signify that there is no correlation between them. We find $R_{\delta^2,\Omega} \approx 0.84$ and $R_{\delta^2,N_{\mathrm{crossing}}} \approx 0.73$, confirming that the time dependence of Ω and N_{crossing} are significantly correlated with the time dependence of δ^2.

To quantify the number of molecules showing large mobility, we count the number $N_{\mathrm{mobile}}(t,\phi)$ of molecules that move more than twice the value of $\langle\delta^2(t,\phi)\rangle$ in the time interval $[t, t+\phi]$, *i.e.* calculating a dynamical analog of N_{crossing}. We find that, on average, $\langle N_{\mathrm{mobile}}(t,\phi)\rangle \approx 13\%$ of the molecules and that the time dependence of N_{mobile} (see fig. 5(b), red line) shows again a strong analogy with N_{crossing}.

In order to reveal possible spatial correlation, we investigate the location of mobile molecules and of molecules performing structural changes. We find that the number of crossing molecules that are also mobile (as averaged along the simulation) is 2.5 times larger than what it would be expected on a random basis. Additionally, we calculated the (system- and time-averaged) minimum distance, D_{min}, from a crossing molecule to a mobile one (a value that would be zero if all the molecules coincided). We find a value of $D_{\mathrm{min}} = 2.77\,\text{Å}$ (very close to the first oxygen-oxygen neighbor distance), much shorter than the value that would render a random location of the crossing molecules with respect to the mobile ones ($\approx 4\,\text{Å}$). This shows that there exists a clear spatial correlation in the location of the mobile molecules (dynamic heterogeneities) and of the molecules undergoing structural changes. Thus, interestingly, the correlation does not only manifest itself in time but also in space.

Before concluding, a few words relating our results to existing two-state models of water seem worthwhile. Amongst the different two-state models that have been proposed, it is interesting to refer briefly to two different recent descriptions: The mixture model [29, 30] and the two-order-parameter model [31]. While in the first case water is supposed to exist in one of two differently structured motifs (like, for example, LDA and HDA), the second one regards water as a mixture of a few structured locally favored molecular arrangements and an unstructured liquid-like state that can have many different local configurations. Both models consider the existence of a structured state made of one (or few) locally well-arranged molecules. Thus, the main difference consists in the fact that the two-order-parameter model considers an unstructured state consisting of a set of many different configurations, which implies that it possesses a large entropy, while the mixture model considers that such state is rather unique (and not necessarily unstructured but with a local structure different from the other state). The use of the real dynamics to calculate local structure indices, as has been done up to now, does not help much in this respect. This is so since thermally induced distortions of a locally preferred structure can yield an outcome not easily distinguishable from that of a plethora of intrinsically different configurations. Thus, our results based on inherent dynamics (where the randomizing effect of thermal fluctuations is explicitly removed by conducting each configuration to its locally energetically preferred structure or local minimum of the basin of attraction where it belongs) can provide some evidence to add to this discussion. First of all, from the shape of the peaks of fig. 1, it seems that the unstructured (and also the structured state) is not represented by a single unique configuration but rather by many different local configurations. Also interesting is the fact that the position of the structured peak is fairly temperature independent while the position of the unstructured peak moves significantly in the temperature range studied. Thus, these findings are in principle consistent with a structured state that entails the contribution of a few well-defined local configurations and an unstructured state representing a high entropy state arising from many different configurations with no local structural preference.

Another prediction of the two-order-parameter model is that the fraction of the structured component should be described by a Boltzmann factor (where the Boltzmann weight expresses the stabilization due to the hydrogen bond energy of the locally favored well-developed hydrogen bonds structure and the destabilization, proportional to the pressure, coming from the concurrent volume increase [31]). With an analysis similar to that of fig. 4 for the different temperatures under study, we calculated the fraction of structured molecules. The result, as shown in fig. 6 for the temperature regime under study, seems in principle to be consistent with such behavior. However, more extensive work would be necessary in this regard.

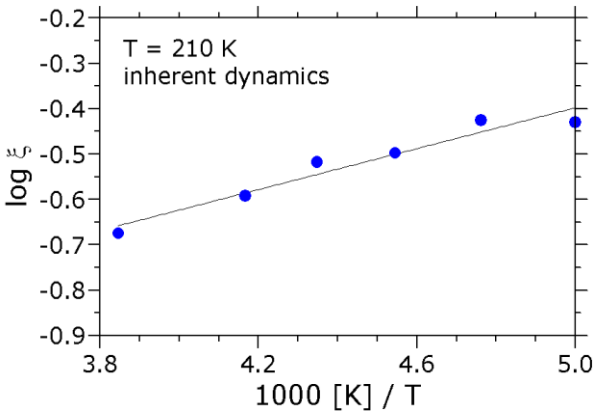

Fig. 6. Arrhenius plot for the fraction of area ξ beneath the structured part of the LSI distribution plot (that of fig. 1) against reciprocal absolute temperature. ξ is evaluated as $\int_{I_{\min}}^{\infty} P(I)\mathrm{d}I$. A linear fit of the data is included, marked by the solid line.

The possibility that the slow dynamics in water and other tetrahedral liquids (instead of stemming from the more generally accepted glass transition scenario) could arise from the competence between the long-range bond and density orderings (as suggested within the two-order parameter model and implying the emergence of an extra energy barrier related to the existence of the structured component [32]), is indeed interesting. We think that in their present state our results, while might aid in the characterization of the structured state, do not add much in this regard. However, further work might be worth pursuing. The usual view we have taken here concerning the dynamics (as, for example, in [17,19]) has in turn many supporting evidences. For example, both the dynamical heterogeneities and the metabasin transitions characterized by relatively compact clusters of mobile particles have been shown to be analogous to the situation in simpler glass-formers–like binary Lennard-Jones systems where the structural details are more trivial [14,19].

4 Conclusions

To summarize, this work demonstrates the validity of a two-state picture of water in a range of temperatures within the supercooled regime. The combined use of ISs and of the LSI indicator shows that supercooled water can be considered as a mixture of "structured" low-local-density and "unstructured" high-local-density molecules. Furthermore, we provide definitive evidence for the connection between structural rearrangements and dynamics: substantial reorganization of structural patterns is demanded if an event relevant to the long-time α relaxation of the system is to take place.

FS acknowledges support from the NoE SoftComp NMP3-CT-2004-502235. Financial support from ANPCyT, SeCyT and CONICET is also gratefully acknowledged. GAA and JARF are research fellows of CONICET.

References

1. P.G. Debenedetti, *Metastable Liquids* (Priceton University Press, Priceton, NJ, 1996).
2. O. Mishima, H.E. Stanley, Nature **396**, 329 (1998).
3. C.A. Angell, Chem. Rev. **102**, 2627 (2002).
4. C.A. Angell, Annu. Rev. Phys. Chem. **55**, 559 (2004).
5. E. Shiratani, M. Sasai, J. Chem. Phys. **104**, 7671 (1996).
6. E. Shiratani, M. Sasai, J. Chem. Phys. **108**, 3264 (1998).
7. O. Mishima, L.D. Calvert, E. Whalley, Nature **310**, 393 (1984).
8. H.-G. Heide, Ultramicroscopy **14**, 271 (1984).
9. T. Loerting, C. Salzmann, I. Kohl, E. Mayer, A. Hallbrucker, Phys. Chem. Chem. Phys. (Inc. Faraday Trans.) **3**, 5355 (2001).
10. T. Loerting, N. Giovambattista, J. Phys.: Condens. Matter **18**, 919 (2006).
11. M.T. Cicerone, M.D. Ediger, J. Chem. Phys. **104**, 7210 (1996).
12. E.R. Weeks, J.C. Crocker, A.C. Levitt, A. Schofield, D.A. Weitz, Science **287**, 627 (2000).
13. S. Glotzer, J. Non-Cryst. Solids **274**, 342 (2000).
14. G.A. Appignanesi, J.A. Rodriguez Fris, R.A. Montani, W. Kob, Phys. Rev. Lett. **96**, 057801 (2006).
15. B. Doliwa, A. Heuer, Phys. Rev. Lett. **91**, 235501 (2003).
16. A. Widmer-Cooper, P. Harrowell, H. Fynewever, Phys. Rev. Lett. **93**, 135701 (2004).
17. G.S. Matharoo, M.S.G. Razul, P.H. Poole, Phys. Rev. E **74**, 050502 (2006).
18. L.O. Hedges, J.P. Garrahan, J. Phys.: Condens. Matter **19**, 205124 (2007).
19. J.A. Rodriguez Fris, G.A. Appignanesi, E. La Nave, F. Sciortino, Phys. Rev. E **75**, 041501 (2007).
20. H.J.C. Berendsen, J.R. Grigera, T.P. Stroatsma, J. Phys. Chem. **91**, 6269 (1987).
21. P.G. Debenedetti, F.H. Stillinger, Nature **410**, 259 (2001).
22. P.-L. Chau, A.J. Hardwick, Mol. Phys. **93**, 511 (1998).
23. J.R. Errington, P.G. Debenedetti, Nature **409**, 318 (2001).
24. Yu.I. Naberukhin, V.P. Voloshin, N.N. Medvedev, Mol. Phys. **73**, 917 (1991).
25. A. Oleinikova, I. Brovchenko, J. Phys.: Condens. Matter **18**, S2247 (2006).
26. F. Sciortino, A. Geiger, H.E. Stanley, J. Chem. Phys. **96**, 3857 (1992).
27. R.A.L. Vallée, M. van der Auweraer, W. Paul, K. Binder, Phys. Rev. Lett. **97**, 217801 (2006).
28. I. Ohmine, J. Phys. Chem. **99**, 6767 (1995).
29. C.H. Cho, S. Singh, G.W. Robinson, Phys. Rev. Lett. **76**, 1651 (1996); J. Urquidi, S. Singh, C.H. Cho, G.W. Robinson, Phys. Rev. Lett. **83**, 2348 (1999).
30. E.G. Ponyatovsky, V.V. Sinitsyn, T.A. Pozdnyakova, JETP Lett. **60**, 360 (1994); E.G. Ponyatovsky, V.V. Sinitsyn, T.A. Pozdnyakova, J. Chem. Phys. **109**, 2413 (1998); E.G. Ponyatovsky, J. Phys.: Condens. Matter **15**, 6123 (2003).
31. H. Tanaka, Phys. Rev. Lett. **80**, 5750 (1998); H. Tanaka, Europhys. Lett. **50**, 340 (2000); H. Tanaka, J. Chem. Phys. **112**, 799 (2000).
32. H. Tanaka, J. Phys.: Condens. Matter **15**, L703 (2003).